LANGMUIR

pubs.acs.org/Langmuir Article

Soap-Film Membranes for CO_2/Air Separation

Céline Hadji, Benjamin Dollet, Benoît Coasne, and Elise Lorenceau*

Cite This: *Langmuir* 2024, 40, 1327−1334 Read Online

ACCESS | Metrics & More | Article Recommendations | Supporting Information

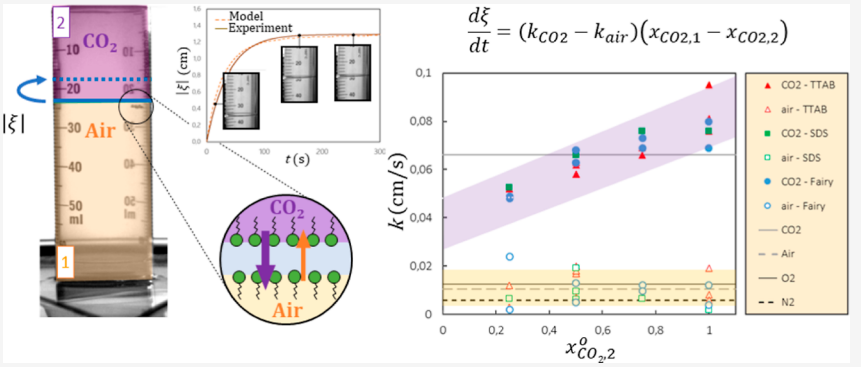

ABSTRACT: Thin liquid films are a potential game changer in the quest for efficient gas separation strategies. Such fluid membranes, which are complementary to their solid counterparts involving porous materials, can achieve complex separation by combining permeability and adsorption mechanisms in their liquid core and at their surface. In addition, unlike porous solid membranes that must be regenerated between separation steps to recover a gas-free porosity, thus preventing continuous operation, liquid membranes can be regenerated using continuous liquid flow through the fluid film. Here, building on the self-sustained mobile film technique, we propose a simple experimental setup allowing direct quantitative assessment of the gas permeability of soap films stabilized by different surfactant types. Using a simple prototypical example involving O_2/N_2 mixtures, the measurement principle is first presented to establish a proof of concept. As the gas solubilities and diffusivities are known, the results of such experiments can be compared with microscopic models to disentangle the liquid core and surface permeabilities from a direct macroscopic transport response of the film subjected to a gas concentration difference. The same dynamical experiments performed for air enriched in CO_2 indicate that the permeability of the soap film varies with the molar fraction in the gas compartment, a feature not observed for O_2/N_2. These experimental findings pave the way for the design of novel separation technologies in fields and situations where porous solid membranes are of limited efficiency.

INTRODUCTION

Gas separation, which encompasses purification and partition operations to obtain single or multiple primary components, is central to applications such as greenhouse gas abatement, air quality control, and filtration from biomass decomposition.[1] While mature technologies are available for large/complex compounds, efficient separation of small molecules such as N_2, O_2, CH_4, CO_2, and H_2 remains challenging as they involve weak and rather unspecific interactions together with light weights—therefore rendering common kinetics or interaction-driven separation of limited efficiency.[2]

Swing adsorption, where one pressurizes and depressurizes a gas stream through a porous solid, is efficient as gases are separated according to their permeability/adsorption properties. Yet, even with the advent of nanoporous materials with tunable chemistry/porosity (e.g., metal−organic frameworks, grafted silica/doped zeolites, and functionalized polymers),[3] such integrated techniques still exhibit limited efficiency for light or weakly interacting species and the design of optimal materials is largely hindered by the unavoidable selectivity/permeability trade-off; large pores lead to efficient transport but poor selectivity and *vice versa* for small pores.[4,5] Moreover, regeneration of the separating host requires costly and complex cycling optimization to recover gas-free porosity between separation steps.

In this context, thin liquid films suspended,[6−8] flowing,[6,9,10] or bubbled onto a solid frame[11] are promising candidates as efficient separation can be achieved by combining complex permeability/adsorption mechanisms in the liquid core and at its surface.[12,13] Moreover, owing to their fluid nature, continuous liquid flow in such films allows permanent

Received: September 27, 2023
Revised: December 15, 2023
Accepted: December 18, 2023
Published: January 3, 2024

https://doi.org/10.1021/acs.langmuir.3c02915
Langmuir 2024, 40, 1327−1334

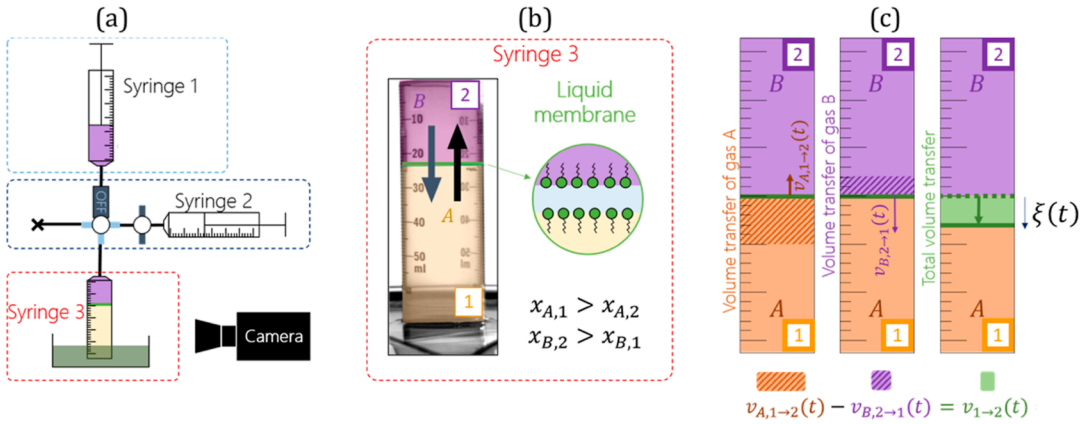

Figure 1. (a) Experimental setup used to prepare the two gas compartments and the soap film in syringe 3. Syringe 1 is used to prepare the gas sample B injected into the upper compartment (compartment 2) while syringe 2 is used to generate and move the soap film prior to gas injection into compartment 2. (b) Zoom-in of syringe 3 where the gas compartments 1 and 2, separated by a liquid membrane composed of water and surfactants, have different compositions. As a result of the gas transfer tending to equilibrate the compositions, the soap film moves up or down. V_1^0 and V_2^0 denote the initial volumes of compartments 1 and 2, respectively. (c) Graphical definition of $v_{A,1\to2}(t)$, the volume of gas A transferred from compartment 1 to 2, $v_{B,2\to1}(t)$, the volume of gas B transferred from compartment 2 to 1, and $v_{1\to2}(t)$, the total volume of gas transferred from compartment 1 to 2. The latter is directly linked to ξ, the film displacement, which is the only experimentally measurable variable.

regeneration by maintaining the gas concentration low and compensating for the small surface area. Among liquid membranes, the use of surfactant-stabilized films such as soap films for gas separation remains largely unexplored despite several ingenious sparse studies.[11,14,15] Yet, surfactant-stabilized soap films offer the following advantages over pure liquid films: (1) improved mechanical stability, (2) limited aging due to reduced evaporation,[16] (3) submicron liquid thicknesses and therefore high permeabilities,[17] and (4) possibility of destroying/reforming the film for complete regeneration.

To go beyond the proof of concept and separate gases by soap films, the efficiency of the process and therefore the permeability of the soap films to all gaseous species considered must be known. In general, permeabilities are measured *globally* by following the evolution of an overpressurized gas volume containing the gas of interest separated from the atmosphere by a soap film. This technique has been used in the geometry of a bubble[7,12,13,16−27] or of a cylinder with a vertical film.[14,15,28,29] The permeabilities deduced using this method, which have been found to depend on temperature,[20] surfactant size/concentration,[16,23] and gas type,[24,25,30] are often only qualitative as the film thickness is often heterogeneous and not controlled. Tock and co-workers also used a vertical film formed in a tube but subjected to a gas concentration difference rather than a pressure difference.[14,15] By using a mobile film, the pressure on either side of the film is equal at all times so that the film is flat, and the gas transfer only occurs because of the gas partial pressure difference with a permeability given by the film displacement as a function of time. Yet, the permeability for a given gas showed unexpected variations, by a factor of up to 10, depending on the nature of the second gas (despite the use of ideal mixtures). Such deviations are thought to be due to large film thickness variations during the measurement arising from film gravity drainage with this vertical geometry. Permeability measurements from the *local* thickness profile of the film between two microbubbles of different volumes have also been carried out recently using an AFM.[17] A good agreement between global and local permeability measurements is reported for microbubbles in simple liquids. However, for liquids containing surfactants or polymers, subtle physicochemical effects of exacerbated solubility or interface permeability are highlighted.[17]

Measuring the permeability of a soap film to a gas can, therefore, be a delicate operation. In this work, we report a simple experimental procedure that enables accurate and robust permeability measurement of self-sustained soap films to various gases without requiring the use of an AFM. This approach is reminiscent of the mobile film technique,[14,15] but with a horizontal film of a known thickness h and with limited kinetic drainage. Moreover, as the permeability of the same film to two different gases can be measured simultaneously, this setup makes it possible to establish a quantitative comparison with microscopic models in which the soap film is represented as a central liquid layer of thickness e sandwiched by two surfaces constituted by surfactant monolayers. To establish a proof of concept, we first consider below thin liquid films stabilized by three surfactant types in contact with O_2/N_2 mixtures of different compositions on either side. For this simple system, the liquid core and surface contributions to the permeability can be inferred readily as the film thickness and gas solubilities are known. As expected for parallel layers, the liquid core and surface permeabilities add up. To illustrate the potential applications of such thin liquid membranes, we also consider a more practical situation in which the same films are subjected to air enriched in CO_2. In contrast to the case for the O_2/N_2 mixtures, there is a deviation from the expected permeability corresponding to the sum of the constant contributions from the liquid core and the surface. This discrepancy probably reveals the subtleties of the interactions between CO_2 and the different elements of the film.

RESULTS

Permeability and Solubility of Soap Films. The gas permeability of a flat horizontal soap film separating two gaseous compartments is measured using the experimental setup shown in Figure 1a. In all experiments, the two compartments are filled with the same gas mixture—either

https://doi.org/10.1021/acs.langmuir.3c02915
Langmuir 2024, 40, 1327−1334

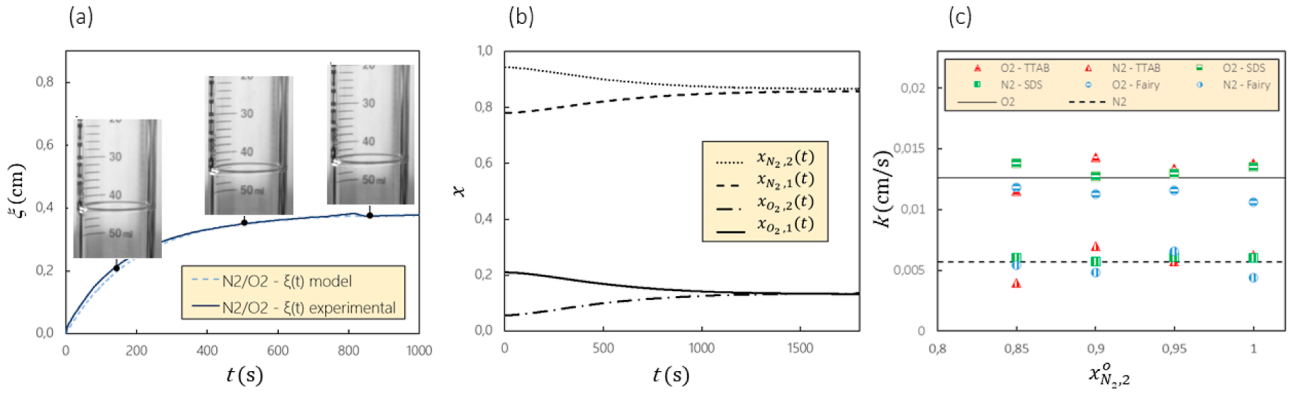

Figure 2. (a) Time evolution of position $\xi(t)$ for a horizontal soap film separating two compartments filled with O_2/N_2 mixtures but with different molar fractions. Our model (black line; see Supporting Information for its analytical expression) provides an accurate description of the experimental results shown as red dots. Initially, compartment 2 is filled with 40 mL of N_2 while compartment 1 is filled with a mixture of O_2/N_2 corresponding to air. (b) Time evolution of the N_2 and O_2 molar fractions in compartments 1 and 2. The initial conditions are V_1^0 = 40 mL, V_2^0 = 40 mL, and $V_{A,1}^0$ = 30 mL. The mole fractions evolve through N_2 and O_2 transfers which drive the system to equilibrium. (c) O_2 (red symbols) and N_2 (blue symbols) permeabilities k of a common black liquid film for various surfactants (from top to bottom: SDS, TTAB, and Fairy) as a function of the N_2 initial molar ratio $x^0_{N_2,2}$.

O_2/N_2 or CO_2/air—but with different compositions. To realize an experiment, we proceed as follows. First, the soap film is generated in air by withdrawing a 50 mL Hamilton glass syringe (syringe 3 in Figure 1a) from a foaming solution containing water and a surfactant. For the surfactants, we either used SDS (surfactant sodium dodecyl sulfate) or TTAB (tetradecyltrimethylammonium bromide) or Fairy which is a commercial surfactant. The compositions of the different foaming solutions are given in the Supporting Information. The soap film is then brought to the top of syringe 3 by withdrawing the air above the film by using syringe 2. Last, syringe 3 is placed vertically with its lower end immersed in a tank containing the soap solution. At this stage, both the bottom and top compartments separated by the soap film in this syringe, referred to as compartments 1 and 2, respectively, are filled with air at ambient pressure. Syringe 1 is used to modify the gas composition in compartment 2 by injecting either pure N_2 in case of O_2/N_2 mixtures or CO_2 in case of CO_2/air mixtures. Before filling compartment 2, the film is kept at rest to ensure that the film has reached its equilibrium thickness, which occurs in 100 s (see Supporting Information). Then, compartment 2 is set in contact at a time t = 0 with the soap film by opening the valve and pushing syringe 1. The vertical film displacement $\xi(t)$ within syringe 3 induced by the gas transfer is monitored with a CCD camera recording 1 and 10 frames/s for the O_2/N_2 and CO_2/air experiments, respectively. All details can be found in the Supporting Information.

By assuming Fickian gas transfer and ideal gas behavior and neglecting viscous friction along the syringe as justified in the Supporting Information section, the film permeability k_G to a given gas G = A or B of a mixture A/B can be inferred from the film displacement ξ as follows. As illustrated in Figure 1b,c, at a given time t, the volume, the number of moles, the concentration, and the molar fraction of gas G in compartment 1 are, respectively, $V_1(t)$, $n_{G,1}(t)$, $c_{G,1}(t)$, and $x_{G,1}(t)$, while $V_{G,1\to m}(t)$ corresponds to the total volume of gas G transferred from compartment l to compartment m, after a time t.

In the framework derived below, ξ, k_G, $V_1(t)$, $n_{G,1}(t)$, $c_{G,1}(t)$, $x_{G,1}(t)$, and $V_{G,1\to m}(t)$ are variables, which depend on t. Yet, for the sake of clarity, we do not write explicitly this temporal dependency in the following framework discussed below. Also, when referring to variables taken at the beginning ($t \to 0$) and at the end ($t \to \infty$) of the experiment, the superscripts 0 and ∞ are used. The experiment can be considered as isothermal (thermodynamic equilibrium is reached instantaneously) and isobaric (the pressure remains identical in the whole system during the experiment as evidenced by (i) the shape of the film that remains flat and (ii) the level of liquid in syringe 3 that remains constant), and the ideal gas approximation will be used at all times t: $V_{G,1} = n_{G,1}RT/P$ where P, T, $V_{G,1}$ and R correspond to the constant pressure, constant temperature, volume occupied by gas G in compartment l, and ideal gas constant.

Within the linear response theory, the liquid membrane permeability k_A defined from the relationship between the concentration difference and the gas transfer rate across the film[13] can be written as

$$\frac{dn_{A,1\to 2}}{dt} = k_A S(c_{A,1} - c_{A,2}) \quad (1)$$

where $n_{A,1\to 2}$ is the number of moles of gas A diffusing through the liquid membrane of constant area S from compartment 1 to compartment 2, and $c_{A,1}-c_{A,2}$ is the concentration difference of gas A in compartments 1 and 2, assumed instantaneously equilibrated, hence uniform in each compartment. With this definition, the permeability $k_A(t)$ has the dimension of a velocity and therefore differs from the permeability in surface area units often used for fluid transport in porous media. Using the ideal gas law, $n_{A,1\to 2} = Pv_{A,1\to 2}/RT$ and introducing the molar fraction of gas A in compartment 1, $x_{A,1} = n_{A,1}/(n_{A,1} + n_{B,1})$, the concentration difference across the two compartments can be expressed as $\Delta c_A = c_{A,1} - c_{A,2} = (P/RT) \times \Delta x_A$ with $\Delta x_A = x_{A,1} - x_{A,2}$. With these considerations, eq 1 becomes $dv_{A,1\to 2}/dt = k_A S \Delta x_A$. Because this last equation also applies to gas B with k_B and $\Delta x_B = x_{B,1} - x_{B,2}$, the total gas transfer $v_{1\to 2}$ can be expressed as

$$\frac{dv_{1\to 2}}{dt} = \frac{dv_{A,1\to 2}}{dt} + \frac{dv_{B,1\to 2}}{dt} = k_A S \Delta x_A + k_B S \Delta x_B$$

Finally, by noting that $\Delta x_A(t) = -\Delta x_B(t)$ because the overall number of molecules is constant and $dv_{1\to 2}/dt = -dV_1/dt =$

https://doi.org/10.1021/acs.langmuir.3c02915
Langmuir 2024, 40, 1327−1334

dV_2/dt with $V_1(t)$ and $V_2(t)$, the volume of compartment 1 and 2, eq 2 can be rewritten as

$$\frac{dV_1}{dt} = -\frac{dV_2}{dt} = (k_B - k_A)S\Delta x_A \quad (2)$$

The last equation is very important as it provides a means to measure at each time the difference of permeabilities $k_B - k_A$ from the initial evolution of film displacement $d\xi/dt = (1/S)dV_1/dt$ (we recall that S is the section area of the film). In what follows, we assume constant permeabilities k_B and k_A during the experiment. The validity of this assumption will be discussed below. Then, the permeability ratio k_A/k_B can be determined from the final film position, as detailed in the Supporting Information section. Then, knowing the difference and the ratio of k_A and k_B, we quantified the two permeabilities for each experiment.

To improve the accuracy of our data analysis, we interpolate the entire $\xi(t)$ curve by a theoretical equation obtained by writing mass conservation for both gases and the equation of state for perfect gases, as explained in the Supporting Information section. A typical $\xi(t)$ curve is displayed in Figure 2a for the experimental measurements corresponding to O_2/N_2. The displacement kinetics is initially very fast but then slows down until the film stabilizes at a given stationary position after ∼20 min (as will be discussed later, much faster kinetics are observed for CO_2/air mixtures with characteristic times of a few minutes only). The data $\xi(t)$ can be used to extract the final displacement ξ^∞ by averaging the ten last data points and calculating $V_1^\infty = V_1^0 - \nu_{1\to2}^\infty$ with $\nu_{1\to2}^\infty = S\xi^\infty$ (see Supporting Information). Assuming constant permeabilities over time, we can then calculate k_B/k_A. Once it is known, $\xi(t)$ can be fitted to determine $k_A - k_B$ (see Supporting Information). This procedure yields the fitted dashed curve in Figure 2a, which accurately matches the experimental data. These data can also be used to infer the evolution of the partial pressure or molar fraction for each gas in the two compartments. As expected, such data displayed in Figure 2b show that the system evolves until the partial pressures of the two gases match those in the two compartments. All experiments reported in this paper were repeated three times to get average permeabilities with an error bar corresponding to the statistical dispersion between the data sets.

N_2/O_2: Surface versus Core Permeabilities. In this section, compartment 2 is filled with a mix of air and N_2 of varying proportions, giving an initial N_2 molar fraction $x^o_{N_2,2}$ between 0.78 and 1, while compartment 1 is filled with air only, i.e., $x^o_{N_2,1} = 0.78$. The N_2 and O_2 permeabilities for the three different foaming solutions are measured as described before and are gathered in Figure 2c. No significant dependence on $x^o_{N_2,2}$, the initial N_2 concentration in compartment 2 is observed. This validates *a posteriori* the use of a linear relationship in the definition of permeability given in Supporting Information. This also shows that there is a limited accumulation of N_2 and O_2 molecules in the liquid core or within the surfactant layers (because large solubilities would affect the transport properties of these different elements). The permeabilities k_{N_2} and k_{O_2} averaged over different initial N_2 concentrations are summarized in Table 1. For a given gas, the permeability barely depends on the nature of the surfactants despite the significant differences between the foaming agents (in particular, SDS and TTAB carry opposite electrostatic charges). This result can be rationalized by the fact that the O_2 and N_2 molecules do not have dipole moments and are, therefore, only weakly sensitive to surfactant charges.

Table 1. O_2 and N_2 Permeabilities of Thin Soap Films Stabilized by Different Foaming Solutions[a]

	TTAB (%)	SDS (%)	*Fairy* (%)
k_{N_2} (cm/s)	0.0058 ± 22	0.0060 ± 10	0.0053 ± 18
k_{O_2} (cm/s)	0.0131 ± 9	0.0133 ± 8	0.0113 ± 13
$\alpha^{-1} = k_{O_2}/k_{N_2}$	2.37 ± 0.37	2.22 ± 0.10	2.21 ± 0.30

[a]For each gas, the permeability given in cm/s and their ratio α^{-1} are obtained using the procedure described in the text.

The soap films considered here are common black films (CBFs) as they have thicknesses $e > 50$ nm.[31] Thus, they can be pictured as a central liquid layer of thickness e sandwiched by two surfaces composed of surfactant monolayers.[13,16,19] With such a geometry, the film permeability k for a given gas can be expressed as a combination in a series of these different layers

$$\frac{1}{k} = \frac{1}{H}\left(\frac{e}{D} + \frac{2}{k^{ML}}\right) \quad (3)$$

where H is Henry's coefficient characterizing the dissolved gas concentration C as compared to its concentration c in the gaseous compartment: $C = Hc$, while D/e, also denoted as k^{LC} so that $k^{LC} = D/e$, is the liquid core permeability—merely a consequence of the gas diffusivity D through the thickness e of the liquid—while k^{ML} is the surface permeability due to the surfactant monolayers. The eq 3 allows us to justify *a posteriori* the hypothesis of constant permeability which implies that e the thickness of the film, D the diffusion coefficient, and H the solubility of the film are all constant. This is a reasonable hypothesis for e, since the thickness of the film stabilizes in around a hundred seconds, which corresponds to the waiting time before starting the experiment, and for D which has little reason to vary. This is less obvious for H, which corresponds to the ratio of liquid and gas phase concentrations, as discussed in the last section of this work.

To go one step further, we compare the values obtained above with the predictions of eq 3. This requires knowing the value of k^{ML}, yet measurements of this parameter are rare. By adding salt to the foaming solution to vary the ionic strength and therefore the thicknesses of the films, Krustev et al. showed that the monolayer permeability of SDS common black films to air is gigantic, constant, and in the order of 0.15 m/s. Note that the definition of k^{ML} used in this work differs by a factor H from that of Krustev et al., which explains why the values mentioned here are not directly comparable with those of their articles.[21,22] The formalisms are equivalent, and we have chosen the definition initially proposed by Princen.[13,19] For comparison, a typical value of the whole permeability of CBFs is in the order of $k \sim 10^{-3}$ m/s.[21,22] More recently, a simultaneous comparison of the overall bubble deflation rate and film thickness using AFM showed a monolayer resistance equal to zero, which also corresponds to a gigantic value of k_{ML}. We thus first neglect the surface contribution ($1/k^{ML} = 0$) and look at the contribution of the liquid core only. We also recall that the two permeability values are obtained in the scope of the same experiment; this implies that the film thickness e in the expression given in eq 3 is identical for the two gases. Then, eq 3 yields $k_{O_2}/k_{N_2} = (H_{O_2}/$

https://doi.org/10.1021/acs.langmuir.3c02915
Langmuir 2024, 40, 1327−1334

$H_{N_2}) \times (D_{O_2}/D_{N_2}) = 2.2$ using the available values from the literature. This is only slightly less than that measured for the three surfactants: on average, we measure $k_{O2}/k_{N2} = 2.26 \pm 0.26$. (see Table 1). This shows that when O_2 and N_2 are separated by a soap film stabilized by TTAB, SDS, or Fairy, the resistance to gas flow in the geometry of our setup is mainly provided by the liquid core ($2/k^{ML} \ll e/D$). However, as we systematically obtain a value of k_{O_2}/k_{N_2} slightly higher than the theoretical value for all our experiments, we interpret this systematic deviation by comparing $k_{N_2}^{ML}$ and $k_{O_2}^{ML}$ via a Taylor expansion of k_{O_2} and using eq 3 in the limit where $2/k^{ML} \ll e/D$ and then calculate k_{O_2}/k_{N_2}

$$\frac{1}{2}\left(\frac{H_{N_2}D_{N_2}k_{O_2}}{H_{O_2}D_{O_2}k_{N_2}} - 1\right) = \frac{D_{N_2}}{e}\left(\frac{1}{k_{N_2}^{ML}} - \frac{D_{O_2}}{D_{N_2}}\frac{1}{k_{O_2}^{ML}}\right) \quad (4)$$

Our measurements of k_{O_2}/k_{N_2} are systematically higher than $(H_{O_2}/H_{N_2}) \times (D_{O_2}/D_{N_2}) = 2.2$, thus the left-hand side of eq 4 is always positive. Using the value of D_{O_2}/D_{N_2} in Table 2, we therefore obtain for the three surfactants: $k_{N_2}^{ML} < k_{O_2}^{ML}$. This systematic behavior, also observed in other studies,[12,24,30] is thought to stem from structural differences between the two molecules. Neither N_2 nor O_2 bears charge or a dipolar moment, yet their diameters and quadrupolar moments are slightly different. A smaller size should logically promote greater permeability because the probability of opening a cavity and allowing a passage through the surfactant layer is increased. Yet, since the diameter of O_2 is slightly larger than the one of N_2, the measured differences in permeability are probably due to differences in quadrupolar moments. N_2 having a greater quadrupolar moment than O_2 will interact more with the charged surfactants, therefore reducing the transfer kinetics despite its smaller diameter. This interpretation, which must be confirmed using numerical simulations, for instance, illustrates the good sensitivity of our experiment. In particular, our setup yields precise quantitative estimates of the permeability of a single molecule, while avoiding difficulties linked to the influence of thickness on permeability.

Table 2. Henry and Diffusion Coefficients for Different Gases[30,32,a]

	H (1)	D ($\times 10^{-9}$ m^2/s)
O_2	3.2×10^{-2}	2.1
N_2	1.6×10^{-2}	1.9
CO_2	8.4×10^{-1}	1.9
air	1.9×10^{-2}	1.9

[a]For O_2, N_2, and CO_2, values were taken from the literature. For air, we use a mean value calculated using the molar percentage of N_2 and O_2 in air.

CO_2/Air. The upper compartment 2 is now initially filled with a mix of air and CO_2, and the bottom compartment 1 with air only. We then observe that the soap film moves upward rather than downward, resulting in negative values of ξ. This suggests that the permeability of CO_2 in the film is greater than that of air. As for the mixtures of N_2 and O_2 studied in the previous section, we extract the permeabilities to CO_2 and air—considering air as an effective gas by itself—for the three studied surfactants from data such as those in Figure 3a. Figure 3b shows the permeability to CO_2, k_{CO2}, and air, k_{air}, of soap films as a function of $x^0_{CO_2,2}$ (i.e., the initial molar fraction of CO_2 in compartment 2). The order of magnitude of k_{air} is ~0.01 cm/s. This value lies between those measured for pure O_2 and N_2 as expected since air is mainly composed of these two gases. In contrast, k_{CO2}, which ranges between 0.045 to 0.095 cm/s, is much larger. This is mostly due to the high solubility of CO_2 in water compared to those of O_2 and N_2 (see Table 2). This high permeability, which ensures a large concentration of dissolved CO_2 in the liquid core, also explains why equilibrium is reached after a few minutes instead of about 1 h in the case of mixtures of N_2 and O_2 (see Figures 2a and 3b). As for O_2/N_2, the permeability of the soap films to CO_2 or air does not depend on the nature of the surfactants. Figure 3

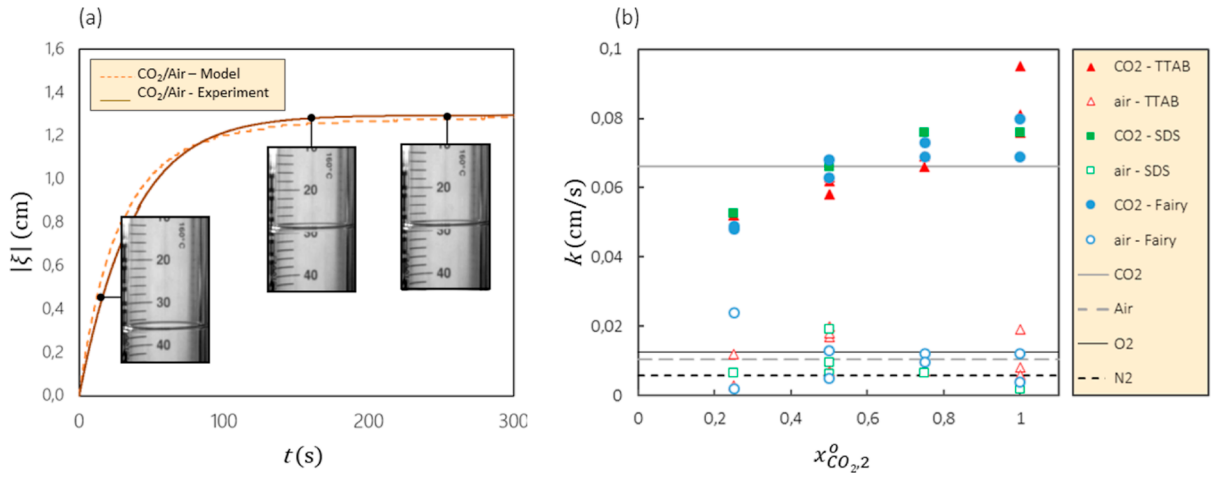

Figure 3. (a) Time evolution of the absolute value of the position $|\xi|$ for a horizontal soap film separating two compartments filled with CO_2/air mixtures with different molar fractions. Like for O_2/N_2 mixtures in Figure 2, our model (black line—see the Supporting Information for the analytical expression) provides an accurate description of the experimental results shown as red dots. Initially, compartment 2 is filled with 20 mL of air and 20 mL of CO_2, while compartment 1 is filled with air only. (b) CO_2 and air permeabilities, k, as a function of the initial CO_2 molar fraction in compartment 2 $x^0_{CO_2,2}$. The results are shown for films stabilized using the three surfactants considered in this study. The permeabilities of air, which are given as a reference, are not permeabilities *per se* but are a combination between the N_2 and the O_2 permeabilities.

https://doi.org/10.1021/acs.langmuir.3c02915
Langmuir 2024, 40, 1327−1334

also reveals that contrary to O_2/N_2 mixtures, the permeability to CO_2 depends on the initial conditions: it increases as the initial molar fraction $x^i_{CO_2,2}$ of CO_2 in compartment 2 increases.

To go one step further, we compare the contribution of the liquid core only neglecting the influence of the surface permeability ($1/k^{ML} = 0$) as previously done for O_2/N_2. Equation 3 and the values in Table 2 give $k_{CO_2}/k_{air} = (H_{CO_2}/H_{air})(D_{CO_2}/D_{air}) = 44.2$. Contrary to what was observed for O_2/N_2, this value is much higher than that obtained experimentally. Indeed, averaging over all our data (regardless of the surfactant and initial molar fraction $x^o_{CO_2}$), we find a smaller value of $k_{CO_2}/k_{air} = 10.1 \pm 8.69$. To conclude, two points are worth noting for CO_2/air: (*i*) the ratio of experimental permeabilities is 4 times smaller than expected and (*ii*) the measured values are highly dispersed as evidenced by a standard deviation of 8.69.

DISCUSSION

The data obtained in this work are two kinds. First, for O_2/N_2, the measurements are surprisingly reproducible and in good agreement with theory. The quantitative comparison of the data with the sandwich model corresponding to eq 4 suggests that the transfer kinetics for these two gases is limited by diffusion through the aqueous core of the soap film (in other words, the contributions of the surfaces to the permeability are of the second order). This ensures that the permeability measurement method described in this work is robust and consistent for both O_2 and N_2. For CO_2/air, the permeability to air, k_{air} also gives a reasonable value, albeit somewhat small. The deviations from theory may be due to the fact that air is a mixture mainly composed of O_2 and N_2 whose transfer kinetics through the soap film are not equivalent. It may appear that the fastest gas, *i.e.*, O_2, contributes the most to the kinetics of transfer as also observed for bubbles degassing inside a hydrogel.[33] A second explanation could come from a limitation of the kinetics by diffusion of the gas itself within the compartment. We assumed that gas concentrations near the membrane are exactly those initially imposed in the compartments. This is true for the very first instants, but the transfer of molecules on either side of the membrane quickly induces an inhomogeneous concentration in the gas compartment. As a result, on the one hand, the concentration of CO_2 in compartment 2 in the vicinity of the membrane is smaller than expected; on the other hand, its concentration in compartment 1 in the vicinity of the membrane is higher than expected. Overall, the driving gradient Δx_{air} would be smaller, thus leading to slower kinetics and an apparent smaller value of k. This phenomenon, known as the concentration polarization effect, is well-known in membrane technologies with liquids, which are used to separate ions from a liquid for water desalination or to recover osmotic energy from concentration gradients. For gases, this effect must be less limiting since the order of magnitude of molecular diffusion in gas is 10^4 times higher than that in a liquid—$D^{CO_2}_{air} \sim 10^{-5}$ m^2/s $\gg D^{CO_2}_{W} \sim 10^{-9}$ m^2/s. Using the data in Figures 2 and 3, a quick estimation of the order of magnitude can be done: for O_2/N_2, the diffusion will homogenize concentration gradients over a size of 0.5 cm (corresponding to the displacement of the membrane in Figure 2) in 2.5 s, which is much less than the total time of the experiment (of the order of 1000 s). For air/CO_2, the displacement of the membrane is twice larger; thus, the typical time for homogenization by diffusion in the gas compartment is 10 s, while the experiment lasts typically 100 s. The diffusion in the gas may well contribute to the slowing down of the general kinetics, which would lead to an apparent decrease of k.

The measurements of k_{CO_2}, the permeability of the soap films to CO_2, are more surprising. First, the data are systematically lower (by a factor on the order of 4) than those predicted by the model. We recall that the model simply takes into account the solubility and diffusion in the aqueous core of the film for the three considered surfactants. This could be due to a kinetic limitation induced either by the polarization of the gas concentration in the two compartments (as already discussed for air) or by the reaction time of solubilization of CO_2 in water. Indeed, the pH of the soap film, initially 7, is acidified by CO_2. For pH < 7, dissolved CO_2 is mainly in the form of H_2CO_3 and HCO_3^-, and the associated dissociation reactions can be slow with a typical reaction time of 25 s.[34,35] Second, we observe a surprising dependence of the permeability on the initial molar fraction of CO_2, which is not observed for air. These variations can either be due to surface contributions to permeability, which would no longer be negligible here. The permeability increase with the initial molar fraction is probably a signature of an interaction between CO_2 molecules and surfactant molecules in the bilayer. Such specific interactions were observed on the same setup with fluorinated gases insoluble in the aqueous core of the film.[31,36] However, for fluorinated gases, the opposite trend was observed: permeability decreases with an increase in the initial molar fraction of gas due to greater adsorption of the gas onto the film.[31] Several studies in the literature, reporting interactions between CO_2 molecules and self-organizing bilayers, provide evidence for complex physicochemical interactions between CO_2 and self-assembled membranes. Tuning the CO_2 concentration in the solution can indeed induce transitions between lamellar and micellar phases of the AOT surfactant,[37] enhance water solubility in alkane by controlling the stability of reverse micelles of Triton X-100,[38] or change the membrane fluidity of the liposome system.[39] From these studies, two mechanisms can be considered to explain our observations. First, pH modification associated with the increase in dissolved CO_2 in the liquid core can modify the permeability of the membrane via a change in the interaction between the charged surfactant heads. Then, since CO_2 molecules are small and very soluble in hydrocarbons, they can accumulate between the hydrocarbon tails of the surfactants and, hence, modify the organization of the self-assembled structure. This hypothesis has recently been confirmed numerically for the AOT lamellar bilayer in water.[40] Anyhow, in the two cases, the average area per surfactant molecule would increase, therefore, increasing in turn the monolayer permeability.

CONCLUSIONS

The simple device described in this paper allows quantitative measurements of the gas permeability of soap films, which is a necessary step for dimensioning a membrane made from a soap film. We obtain robust results for O_2/N_2, which highlight that the permeability for these two gases is limited by diffusion in the aqueous core (the contribution of the surfactants is found

https://doi.org/10.1021/acs.langmuir.3c02915
Langmuir 2024, 40, 1327−1334

to be of second order). Thanks to a Taylor expansion, we also infer that O_2 is more likely to interact with the dense layer of surfactants due to a larger quadrupolar moment. The equivalent thickness measurements are also consistent with the drainage kinetics of the film. The robustness of the results obtained for O_2 and N_2 therefore makes it possible to go a step further and work with more complex gases such as CO_2 and simultaneously measure the permeability of the gas of interest and the thickness of the film via the permeability of the reference gas. In the present paper, this is tested with CO_2/air—air being our reference gas. The permeabilities of the reference gas (air) and the gas of interest (CO_2) are both lower than expected, presumably due to gas diffusion limitations. However, there is also a variation in the CO_2 permeability with the initial molar fraction of gas, which is likely a signature of an interaction of this gas with the monolayer.

Such physicochemical interactions between molecules in the gas phase and the liquid—air interface have been observed via sophisticated techniques, such as X-ray or neutron scattering. In particular, hexane molecules from the vapor phase can adsorb on a gas/liquid interface stabilized by film surfactants reaching a ratio of adsorbed alkane per surfactant molecules between 0,5, and 6, depending on the nature, concentration, and hydrophobic tail length of the surfactant.[41] To the best of our knowledge, such measurements have not been carried out with CO_2. This would make it possible to obtain additional reliable and quantitative data on the interaction between CO_2 molecules and the air/liquid interface. However, these techniques are not easily accessible, and counting times are often long to obtain reliable data.

■ ASSOCIATED CONTENT

Supporting Information

The Supporting Information is available free of charge at https://pubs.acs.org/doi/10.1021/acs.langmuir.3c02915.

Chemical composition and origin of the aqueous solutions and gases used, film thickness measurements, procedure used to limit drainage, theoretical expression used to describe the curves, and discussion of why friction is negligible (PDF)

■ AUTHOR INFORMATION

Corresponding Author

Elise Lorenceau − *Univ. Grenoble Alpes, CNRS, LIPhy, Grenoble 38000, France;* orcid.org/0000-0001-6511-2212; Email: elise.lorenceau@univ-grenoble-alpes.fr

Authors

Céline Hadji − *Univ. Grenoble Alpes, CNRS, LIPhy, Grenoble 38000, France*

Benjamin Dollet − *Univ. Grenoble Alpes, CNRS, LIPhy, Grenoble 38000, France;* orcid.org/0000-0002-1756-7543

Benoît Coasne − *Univ. Grenoble Alpes, CNRS, LIPhy, Grenoble 38000, France;* orcid.org/0000-0002-3933-9744

Complete contact information is available at: https://pubs.acs.org/10.1021/acs.langmuir.3c02915

Notes

The authors declare no competing financial interest.

■ ACKNOWLEDGMENTS

The authors are grateful to Sylvie Spagnoli, Thibaut Metivet, and Thomas Combriat for providing spectroscopic measurements and performing data computation and to Cécile Aprili for fruitful discussion. This work was partially supported by the LabEx Tec 21 (Investissements d' Avenir—grant agreement no. ANR-11-LABX-0030) and the French National Research Agency in the framework of the "Investissement d'avenir" program (ANR-15-IDEX-02).

■ REFERENCES

(1) Sholl, D. S.; Lively, R. P. Seven chemical separations to change the world. *Nature* **2016**, *532*, 435−437.

(2) Lin, J. Y. S. Molecular sieves for gas separation. *Science* **2016**, *353*, 121−122.

(3) Koros, W. J.; Zhang, C. Materials for next-generation molecularly selective synthetic membranes. *Nat. Mater.* **2017**, *16*, 289−297.

(4) Robeson, L. M. The upper bound revisited. *J. Membr. Sci.* **2008**, *320*, 390−400.

(5) Park, H. B.; Kamcev, J.; Robeson, L. M.; Elimelech, M.; Freeman, B. D. Maximizing the right stuff: The trade-off between membrane permeability and selectivity. *Science* **2017**, *356*, No. eaab0530.

(6) Krull, F. F.; Fritzmann, C.; Melin, T. Liquid membranes for gas/vapor separations. *J. Membr. Sci.* **2008**, *325*, 509−519.

(7) Reznickova, J.; Petrychkovych, R.; Vejrazka, J.; Setnickova, K.; Uchytil, P. Gas separation ability of the liquid bubble film. *Sep. Purif. Technol.* **2016**, *166*, 26−33.

(8) Farajzadeh, R.; Barati, A.; Delil, H. A.; Bruining, J.; Zitha, P. L. J. Mass transfer of CO2 into water and surfactant solutions. *Pet. Sci. Technol.* **2007**, *25*, 1493−1511.

(9) Setnickova, K.; Sima, V.; Petrychkovych, R.; Reznickova, J.; Uchytil, P. Separation of gas mixtures by new type of membranes − Dynamic liquid membranes. *Sep. Purif. Technol.* **2016**, *160*, 132−135.

(10) Uchytil, P.; Setnickova, K.; Tseng, H.-H.; Sima, V.; Petrickovic, R. Description of the gas transport through dynamic liquid membrane. *Sep. Purif. Technol.* **2017**, *184*, 152−157.

(11) Lin, Y.-C.; Setnickova, K.; Wang, D. K.; Chu, Y.-F.; Sima, V.; Chiang, Y.-Y.; Uchytil, P.; Tseng, H.-H. Innovative water-based dynamic liquid bubble membrane generation device for gas/vapour separation. *Chem. Eng. J.* **2022**, *450*, 138233.

(12) Ramanathan, M.; Müller, H. J.; Möhwald, H.; Krastev, R. Foam Films as Thin Liquid Gas Separation Membranes. *ACS Appl. Mater. Interfaces* **2011**, *3*, 633−637.

(13) Princen, H.; Mason, S. G. The permeability of soap films to gases. *J. Colloid Interface Sci.* **1965**, *20*, 353−375.

(14) Cook, R. L.; Tock, R. W. Aqueous Membranes for the Separation of Gaseous Mixtures. *Sep. Sci.* **1974**, *9*, 185−193.

(15) Haas, F. W.; Tock, R. W. Permeation of Permanent Gases through Liquid Membranes. *Sep. Sci.* **1975**, *10*, 723−729.

(16) Farajzadeh, R.; Krastev, R.; Zitha, P. Foam film permeability: Theory and experiment. *Adv. Colloid Interface Sci.* **2008**, *137*, 27−44.

(17) Yang, Y.; Biviano, M. D.; Guo, J.; Berry, J. D.; Dagastine, R. R. Mass transfer between microbubbles. *J. Colloid Interface Sci.* **2020**, *571*, 253−259.

(18) Brown, A.; Thuman, W. C.; McBain, J. Transfer of air through adsorbed surface films as a factor in foam stability. *J. Colloid Sci.* **1953**, *8*, 508−519.

(19) Princen, H.; Overbeek, J. T. G.; Mason, S. G. The permeability of soap films to gases. *J. Colloid Interface Sci.* **1967**, *24*, 125−130.

(20) Krustev, R.; Platikanov, D.; Nedyalkov, M. Permeability of common black foam films to gas. Part 2. *Colloids Surf., A* **1997**, *123−124*, 383−390.

(21) Krustev, R.; Platikanov, D.; Nedyalkov, M. Permeability of common black foam films to gas. Part 1. *Colloids Surf., A* **1993**, *79*, 129−136.

(22) Krustev, R.; Platikanov, D.; Stankova, A.; Nedyalkov, M. Permeation of gas through Newton Black Films at different chain length of the surfactant. *J. Dispersion Sci. Technol.* **1997**, *18*, 789−800.
(23) Muruganathan, R.; Müller, H. J.; Möhwald, H.; Krastev, R. Effect of headgroup size on permeability of newton black films. *Langmuir* **2005**, *21*, 12222−12228.
(24) Farajzadeh, R.; Muruganathan, R.; Rossen, W. R.; Krastev, R. Effect of gas type on foam film permeability and its implications for foam flow in porous media. *Adv. Colloid Interface Sci.* **2011**, *168*, 71−78.
(25) Ramanathan, M.; Müller, H.; Möhwald, H.; Krastev, R. Foam films as thin liquid gas separation membranes. *ACS Appl. Mater. Interfaces* **2011**, *3*, 633−637.
(26) Nedyalkov, M.; Krustev, R.; Kashchiev, D.; Platikanov, D.; Exerowa, D. Permeability of Newtonian black foam films to gas. *Colloid Polym. Sci.* **1988**, *266*, 291−296.
(27) Nedyalkov, M.; Krustev, R.; Stankova, A.; Platikanov, D. Mechanism of permeation of gas through Newton black Films at different temperatures. *Langmuir* **1992**, *8*, 3142−3144.
(28) Quoc, P.; Zitha, P.; Currie, P. Effect of foam films on gas diffusion. *J. Colloid Interface Sci.* **2003**, *125*, 1128−1129.
(29) Sujatha, K.; Das, T.; Kumar, R.; Gandhi, K. Permeation of gases through liquid films. *Chem. Eng. Sci.* **1988**, *43*, 1261−1268.
(30) Saulnier, L.; Drenckhan, W.; Larré, P. E.; Anglade, C.; Langevin, D.; Janiaud, E.; Rio, E. In situ measurement of the permeability of foam films using quasi-two-dimensional foams. *Colloids Surf., A* **2015**, *473*, 32−39.
(31) Hadji, C.; Dollet, B.; Bodiguel, H.; Drenckhan, W.; Coasne, B.; Lorenceau, E. Impact of Fluorocarbon Gaseous Environments on the Permeability of Foam Films to Air. *Langmuir* **2020**, *36*, 13236−13243.
(32) Cussler, E. L. *Diffusion: Mass Transfer in Fluid Systems*; 2nd ed.; Cambridge University Press: New York, 1997.
(33) Haudin, F.; Noblin, X.; Bouret, Y.; Argentina, M.; Raufaste, C. Bubble dynamics inside an outgassing hydrogel confined in a Hele-Shaw cell. *Phys. Rev. E* **2016**, *94*, 023109.
(34) Pinsent, B. R. W.; Roughton, F. J. W. The kinetics of combination of carbon dioxide with water and hydroxide ions. *Trans. Faraday Soc.* **1951**, *47*, 263.
(35) House, W.; Howard, J.; Skirrow, G. Kinetics of carbon-dioxide transfer across the air water interface. *Faraday Discuss.* **1984**, *77*, 33−45.
(36) Dollet, B. Coarsening of foams driven by concentration gradients of gases of different solubilities. *Langmuir* **2023**, *39*, 16174−16181.
(37) Zhuo, S.; Huang, Y.; Peng, C.; Liu, H.; Hu, Y.; Jiang, J. CO2-Induced Microstructure Transition of Surfactant in Aqueous Solution: Insight from Molecular Dynamics Simulation. *J. Phys. Chem. B* **2010**, *114*, 6344−6349.
(38) Shen, D.; Zhang, R.; Han, B.; Dong, Y.; Wu, W.; Zhang, J.; Li, J.; Jiang, T.; Liu, Z. Enhancement of the solubilization capacity of water in Triton X-100/cyclohexane/water system by compressed gases. *Chem.—Eur. J.* **2004**, *10*, 5123−5128.
(39) Bothun, G.; Knutson, B.; Strobel, H.; Nokes, S. Liposome fluidization and melting point depression by pressurized CO2 determined by fluorescence anisotropy. *Langmuir* **2005**, *21*, 530−536.
(40) Zhang, J.; Han, B.; Li, W.; Zhao, Y.; Hou, M. Reversible Switching of Lamellar Liquid Crystals into Micellar Solutions using CO_2. *Angew. Chem. Int. Ed.* **2008**, *47*, 10119−10123.
(41) Campbell, R. A.; Kairaliyeva, T.; Santer, S.; Schneck, E.; Miller, R. Direct Resolution of the Interactions of a Hydrocarbon Gas with Adsorbed Surfactant Monolayers at the Water/Air Interface Using Neutron Reflectometry. *Colloids Interfaces* **2022**, *6*, 68.

https://doi.org/10.1021/acs.langmuir.3c02915
Langmuir 2024, 40, 1327−1334